Physiological and proteomic characterization of light adaptations in marine *Synechococcus*

Katherine RM Mackey[1*], Anton F Post[3], Matthew R McIlvin[2], and Mak A Saito[2,*]

[1]Earth System Science, University of California Irvine, Irvine CA 92697

[2]Marine Chemistry and Geochemistry, Woods Hole Oceanographic Institution, Woods Hole MA 02536

[3]Graduate School of Oceanography, University of Rhode Island, Narragansett RI 02882

* corresponding authors, kmackey@uci.edu, 949.824.1133 and msaito@whoi.edu, 508.289.2393

The authors declare no conflict of interest.

This article has been accepted for publication and undergone full peer review but has not been through the copyediting, typesetting, pagination and proofreading process which may lead to differences between this version and the Version of Record. Please cite this article as an 'Accepted Article', doi: 10.1111/1462-2920.13744

Summary

Marine *Synechococcus* thrive over a range of light regimes in the ocean. We examined the proteomic, genomic, and physiological responses of seven *Synechococcus* isolates to moderate irradiances (5-80μE m^{-2} s^{-1}), and show that *Synechococcus* spans a continuum of light responses ranging from low light optimized (LLO) to high light optimized (HLO). These light responses are linked to phylogeny and pigmentation. Marine sub-cluster 5.1a isolates with higher phycouribilin: phycoerythrobilin ratios fell toward the LLO end of the continuum, while sub-cluster 5.1b, 5.2, and estuarine *Synechococcus* with less phycouribilin fell toward the HLO end of the continuum. Global proteomes were highly responsive to light, with >50% of abundant proteins varying more than two-fold between the lowest and highest irradiance. All strains down-regulated phycobilisome proteins with increasing irradiance. Regulation of proteins involved in photosynthetic electron transport, carbon fixation, oxidative stress protection (superoxide dismutases), and iron and nitrogen metabolism varied among strains, as did the number of high light inducible protein (Hlip) and DNA photolyase genes in their genomes. All but one LLO strain possessed the photoprotective orange carotenoid protein (OCP). The unique combinations of light responses in each strain gives rise to distinct photophysiological phenotypes that may affect *Synechococcus* distributions in the ocean.

Introduction

Marine picocyanobacteria are the most abundant oxygenic photosynthetic organisms on Earth. The members of two genera, *Synechococcus* and *Prochlorococcus*, contribute ~25% of net marine primary productivity globally (1), and up to ~80% in the open ocean gyres (2). While light adaptations in *Prochlorococcus* show clear patterns that reflect depth in the water column and taxonomic identity (3–5), light adaptations in *Synechococcus* are more varied and involve a large protein-based light harvesting antenna in addition to chlorophyll (6). Global proteomics provides a new lens to understand how key groups of proteins together give rise to distinct light phenotypes in *Synechococcus*.

In the ocean, *Synechococcus* and *Prochlorococcus* trade off in dominance. The distribution of *Synechococcus* ranges from coastal to open ocean habitats that extend deep into temperate climate zones (1,7–9), whilst *Prochlorococcus* is more abundant in the stratified oligotrophic open ocean within tropical and subtropical latitudes. Where the two genera coexist within stratified waters, they occupy different depth ranges; *Synechococcus* abundances peak in the surface mixed layer and decline at greater depth (3–5,10–12), while *Prochlorococcus* abundances are highest between 20 m and the base of the euphotic zone (~200 m) (Fig. 1A). Typically *Synechococcus* is less abundant below ~100 m, but is occasionally found at depths down to 200-600 m during deep mixing events (12,13), where members of clade I and II can dominate (14).

Given the extensive range of light environments they occupy, it is not surprising that considerable photosynthetic diversity exists between the two genera and even among different ecotypes within the same genus. *Synechococcus* spp. possess multi-protein phycobilisome

antennae that vary in their light harvesting capabilities and spectral properties. Because phycobilisomes constitute up to half of cell protein in cyanobacteria (15–17), they come at a high nitrogen (N) cost for the cells (18). Cells that contain phycocyanin only are green in color and absorb a broad range of orange-red wavelengths. Cells that carry one or more of the phycoerythrin varieties in addition to phycocyanin typically appear as pink or orange-brown in color and preferentially absorb green and blue light (4,19,20). This variation in pigmentation expands the niche for *Synechococcus* by allowing it to access wavelengths of light that other phototrophs cannot, such as under high chlorophyll bloom conditions when a greater proportion of green light is available relative to blue (21).

Various combinations of photoprotective mechanisms exist in different ecotypes of *Synechococcus*. These include (1) reduction in light harvesting antenna size, (2) energy partitioning between photosystem I (PSI) and photosystem II (PSII) via state transitions (22–24), (3) non-photochemical quenching of absorbed energy as heat via the orange carotenoid protein (OCP)(25), (4) accessory antenna formation around PSI by the iron stress induced protein (IsiA)(26,27), and (5) regulation of chlorophyll synthesis, photosystem assembly, and energy dissipation by high light inducible proteins (Hlips)(28–31). Other non-photosynthetic tactics for handling the stress of high light include photolyase activation to mitigate DNA damage (32), and production of various proteins to minimize damage from oxidative stress (33,34). Alternative oxidase pathways and other photorespiratory electron sinks also protect cells from photoinhibition during over-reduced conditions (35–40).

Observations from laboratory experiments (41–44) and field campaigns (6–8,45–47) have together demonstrated that both nutrients and temperature are important drivers in the diversification and biogeography of *Synechococcus* lineages (48). Overlaid on the patterns of

nutrients and temperature in the ocean is the ambient light regime. Spectral quality is a driver of *Synechococcus* pigment diversity (6), but less is known about light intensity. Light, nutrients, and temperature co-vary to different extents in different parts of the ocean, and therefore teasing out the effect of light on *Synechococcus* ecophysiology is complex. Additionally, despite their abundance in surface ocean waters, anecdotal evidence suggests that many cultured *Synechococcus* isolates grow more consistently and are less prone to "crashing" whilst grown under relatively low irradiance of 10-20 μE m^{-2} s^{-1} compared to higher irradiances (J. Waterbury pers. comm.), and certain strains appear to be more robust under higher irradiances. To shed light on photoacclimation responses and light adaptations in *Synechococcus*, we examined the photosynthetic and growth responses of seven strains from different clades to irradiances ranging from 5 to 80 μE m^{-2} s^{-1}. The strains were isolated from different latitudes in the Atlantic Ocean in both open water and coastal environments (Fig. 1B) and encompass different pigment-types. Gene and protein content were compared among the strains, with the goal of improving our understanding of how light intensity shapes the ecophysiology of *Synechococcus* in nature.

Results and Discussion

Proteome responses to irradiance

To understand the protein-based mechanisms that give rise to growth and photophysiology traits in *Synechococcus*, we examined the proteomes of the seven strains, with particular focus on five protein categories: light harvesting, photosynthetic electron transport, carbon fixation, and nitrogen and iron metabolism. Global proteomes (defined here as the untargeted measurement of many proteins simultaneously within an organism) were measured for each *Synechococcus* strain and light intensity, generating 33 global proteomic datasets (Supplemental Tables 2-8). For all

seven strains light intensity caused a strong reshaping of the global proteomes, with >50% of the proteins in each proteome changing more than two-fold between the lowest and highest irradiance levels (Table 1; Supplemental Fig. 1).

Under higher light, phycobilisome proteins involved in light harvesting became less abundant in all strains, consistent with prior observations that phycoerythrin concentrations in strain WH7803 are 20-fold lower in cells grown at 700 $\mu Em^{-2}s^{-1}$ compared to 30$\mu Em^{-2}s^{-1}$ (15). Similarly, photosynthetic electron transport proteins and carbon fixation proteins became less abundant in five and four of the strains respectively (Table 1). This response is consistent with cells requiring less photosynthetic machinery under higher light when photosynthesis saturates more quickly.

Proteins involved in iron and nitrogen metabolism were more abundant in higher light for four and five of the seven strains respectively (Table 1). Both are consistent with a greater need for protein repair and greater metabolic throughput at higher growth rates. The canonical example is the PSII D1 protein (PsbA) that binds the P680 reaction center and other cofactors involved in photosynthetic charge separation, and which is highly susceptible to photodamage (49). Degradation and synthesis of D1 are both photoregulated, and D1 turnover rates are among the highest protein turnover rates in nature (50). The need for repair and synthesis of D1, and other proteins, would increase as photosynthetically-generated reactive oxygen species accumulate, hence the ability to internally recycle nitrogen quickly would be advantageous under higher light (51). Iron proteins like ferredoxins are electron carriers, and their increased abundance (without a concomitant increase in C fixation proteins) may imply a greater capacity for shuttling photosynthetically generated electrons to cellular processes other than carbon fixation (e.g., nitrate reduction). Ferredoxins also facilitate cyclic electron flow around PSI, by which cells generate additional ATP that can be used for protein repair (40). Hence, a higher demand for

cellular maintenance processes under higher light is consistent with the increased levels of iron and nitrogen metabolism proteins observed here.

Photoacclimation and photoprotection traits

Photosynthetic organisms acclimate to light in many ways. There is a distinction between long-term steady-state photoacclimation, which involves tailoring photosynthesis and metabolism to a particular growth irradiance over hours to days, and short-term acclimation that involves activation of temporary processes to cope with fluctuating light (as during rapid mixing or changing cloud cover) (52). While proteins can be involved in these short-term processes, they are more likely to involve activation or relocation of the protein within the cell rather than *de novo* synthesis, which takes place over longer time scales. All cells in this study were cultured under consistent, continuous light, and the acclimation responses discussed here reflect those of steady-state conditions. Below we discuss additional photoacclimation phenotypes and photoprotective responses, while noting that photoprotective responses under fluctuating light regimes could differ from these steady state responses.

Long term (e.g. multi-generation) acclimation characteristics reflect the balance of an organism's investment in certain protein categories (e.g. light harvesting, carbon fixation, N metabolism, etc.). In addition to the categories analyzed in Table 1 and Figs. 4-6, high light inducible proteins (Hlips) play a direct role in photosystem assembly and repair (28,31), dissipating excitation energy within the antenna complexes (29), or regulating chlorophyll synthesis (30). Due to their small size and few resulting tryptic peptides available for detection, Hlips spectra were not abundant in the proteomes presented here, although they are present in the genomes (Supplemental Tables 1-8). To compare the genetic potential of each strain for Hlip production,

we searched for *hli* sequences in each strain's genome (Table 1). This analysis shows that *hli* content varied from 4 to 15 copies per genome across strains and did not show a consistent relationship with strain photophysiology or growth responses to irradiance. The highest *hli* gene content was in the HLO strain WH5701, with 15 *hli* genes, followed by LLO strain WH8020 with 12 *hli* genes. All other strains had ≤9 hli genes (Table 1).

A similar genome analysis was conducted to enumerate photolyase genes. Photolyases are DNA repair enzymes that fix damage caused by ultraviolet light exposure (32). In nature *Synechococcus* photolyase genes are upregulated in midday when light intensity is at its peak (53); however, ultraviolet light was not included as a treatment in this study, and accordingly photolyase proteins were not abundant in the proteomes as measured here (Supplemental Tables 2-8). However, all strains had 3- 5 photolyase genes in their genomes (Table 1). Therefore, while *hli* and photolyase transcripts generally increase with irradiance in certain *Synechococcus* strains (53,54), the numbers of *hli* and photolyase genes in each strain do not appear to be correlated with growth response to irradiance level.

Oxidative stress is a challenge introduced by high light. Reactive oxygen species produced during photosynthesis increase under high light and cause damage to proteins, reducing photosynthetic efficiency. To understand how different strains of *Synechococcus* cope with reactive oxygen species generated during photosynthesis at high light, we compared the abundances of two classes of proteins that protect cells from oxidative stress. The first is the protein Psb28, which assists in PSII assembly, stabilization, and repair following photoinhibition or heat stress (33,55,56). The second class is a group of antioxidant proteins called superoxide dismutases (SODs), which scavenge superoxide radicals generated during photosynthesis (34). SODs are a diverse group of metalloenyzmes utilizing Fe/Mn, Cu/Zn , or Ni cofactors. While

Prochlorococcus uses Ni SOD exclusively (57,58), *Synechococcus* strains can have all three types of SODs with any given strain having one or more type of SOD (e.g. see Fig. 8; Supplemental Table 1). Cu/Zn and Fe/Mn SODs can contain either metal cofactor in the pair (e.g. Cu or Zn, and Fe or Mn), though which metal an organism uses is not obvious from sequence alone (59). Across nearly all strains, these oxidative stress response proteins were generally even or more abundant in higher light (Fig. 8), in keeping with greater oxygen production and oxidative stress during high light exposure. An exception is strain WH5701, where the abundance of both types of SODs declined with increasing irradiance. The reason for this unexpected response is not clear, but could involve alternative antioxidant pathways. Notably, SODs in strains toward the HLO end of the continuum tended to have either manganese or iron cofactors, while strains toward the LLO end of the spectrum tended to have copper/zinc or nickel cofactors (Fig. 8).

Acclimation under fluctuating light requires dynamic photoprotective responses, where cells must efficiently use or discard light energy in real time to avoid photodamage. Photophysiological metrics like fluorescence are useful in understanding these short-term responses. In this study, resilience was assessed by examining the photosynthetic electron transport rate of cells under actinic light levels ranging up to 1000 $\mu Em^{-2}s^{-1}$ (Fig. 3). While photosynthesis in all HLO strains was resilient under this transient high light exposure regardless of growth irradiance, some of the LLO strains were also surprisingly resilient. In particular, strain WH8102 coped well with high actinic light when grown under 40 or 80 $\mu Em^{-2}s^{-1}$ (Fig. 3). This is consistent with prior observations of high photosynthetic efficiency in this strain, and could indicate alternative electron flow pathways are utilized to prevent photoinhibition (36–38).

Cyanobacteria utilize several reversible acclimation strategies to cope with rapid changes in irradiance. The orange carotenoid protein (OCP) binds reversibly to the phycobilisome antenna in a blue-green light dependent manner, and dissipates light energy absorbed by the phycobilisome through fluorescence quenching (25). The amount of quenching, and hence photoprotection, scales with abundance of the OCP (60). All *Synechococcus* strains in this study have the OCP except for the LLO strain WH8109 (Table 1, Supplemental Table 1). Growth in light-limited environments would obviate the need for fluorescence quenching because all of the harvested light would be needed for photosynthesis, perhaps allowing this strain to lose the gene without cost. Overall OCPs were rarely detected in the global proteomes (Supplemental Table 1); however, they were detected in the proteomes of intermediate strain WH7805 and HLO strain PCC7002 (Supplemental Fig. 2). In both cases OCP abundance increased with increasing growth irradiance, consistent with its photoprotective role. The abundance of the OCP could be one factor that determines the ability of cells to maintain high growth rates and avoid photoinhibition during short-term, non-steady state exposure to very high light, such as during mixing, or immediately following stratification before cells are fully acclimated to the new light regime.

Another photoprotective mechanism that reduces the effective cross section (σ_{blue}) of PSII is the state transition, in which the PBS directs excitation energy between PSII and PSI depending on the redox poise of the plastoquinone pool (61). The process is thought to occur either via spillover of energy from PSII to PSI (24), or via movement of the PBS between the two photosystems (22). During a state transition the cell can decrease excitation energy funneled into PSII and channel it toward PSI. Because PSI pulls electrons out of the electron transport chain, this process allows the membrane to remain oxidized and prevents photodamage to PSII. State transitions were apparent in some of the strains tested here, as evidenced by increases in the σ_{blue}

of PSII under dim actinic light relative to dark acclimated cells (23,62)(Fig. 2). The increased cross section in dim light indicates closer PBS affiliation with PSII compared to dark acclimated cells. In the cyanobacteria, photosynthetic and respiratory electron transport occur within the same membrane in *Synechoccocus*. Therefore, cells are expected to be in state II (excitation energy preferentially directed to PSI) in the dark due to the respiratory reduction of the plastoquinone pool. When cells transition from darkness to light, a state I transition occurs (excitation energy preferentially directed to PSII) as photosynthesis causes the membrane to re-oxidize, and affiliation of the PBS with PSII leads to an increase in the effective cross section of PSII (σ_{PSII}). This state transition response was less pronounced in strains that lack phycoerythrin (e.g. WH5701 and PCC7002), possibly because the phycobilisome is considerably smaller and absorbs less blue light if only phycocyanin is present in the PBS. While state transitions are a major mechanism by which *Synechococcus* acclimates to growth at different temperatures (43), they do not appear to become more or less frequent under different growth irradiance (Fig. 2). Rather, the major phycobilisome-based acclimation response to irradiance level appears to be regulation of the amount of pigment protein present in the cell. Indeed, all strains tested here acclimated to higher light by synthesizing less of the proteins that comprise the phycobilisome (Table 1, Fig. 2).

A light response continuum

Based on the above analysis of proteome response, photoprotective genes, and short-term acclimation traits, our findings suggest the light adaptations of *Synechococcus* fall along a continuum, where ecotypes range from low light optimized (LLO) to high light optimized (HLO). Here, we discuss the growth, photophysiology, and associated proteomic responses (light harvesting, photosynthetic electron transport, carbon fixation, and iron and nitrogen metabolism,

Table 1) of each strain in terms of whether they align more closely toward the HLO or LLO ends of a continuum, while demonstrating that considerable diversity exists and many strains share traits from both ends of this continuum.

The strain with the most HLO characteristics examined here was strain WH7803, in keeping with prior observations that it can be cultured under very high irradiances (15). Its growth rate did not saturate in the range of irradiances tested in this study, and continued to increase up to the highest irradiance of 80 $\mu Em^{-2}s^{-1}$ (Fig. 2). This strain maintained high photosynthetic electron transport rates even when acclimated to low light (Fig. 3). Additionally, the majority of proteins involved in major cellular processes like photosynthetic electron transport, carbon fixation, and iron and nitrogen metabolism were generally more abundant in cells acclimated to the highest light level (Fig. 4A, Table 1).

Strain WH5701 also appears suited to a consistently high light environment, showing high photosynthetic electron transport rates and high electron transport protein abundances when acclimated to the highest light treatment (Fig. 3, Fig. 4B). The protein response of this strain was similar to WH7803 except that only slightly more than half (54%) of the Fe-related proteins were more abundant in low light (Fig. 4B, Table 1), suggesting a more moderate response.

The growth rate of strain PCC7002 was the highest of all the strains and did not reach saturation within the range of light intensities we tested (Fig. 2). The photosynthetic electron transport rate for PCC7002 were also the highest observed for all of the strains. But surprisingly, this strain shares many proteome features in common with strains on the LLO end of the light response continuum. For example, PCC7002 proteins in the light harvesting, photosynthetic electron transport, carbon fixation, and nitrogen metabolism categories were more abundant under low

light (Fig. 5A, Table 1). This strain was isolated from a benthic habitat (Table 1) and the LLO characteristics may reflect certain low light adaptations that would be beneficial in a benthic environment.

Strain WH7805 falls squarely in the middle of the light response continuum. Its maximum growth rate occurred at 20 μE m^{-2} s^{-1} (Fig. 2), and it would not grow consistently at 80 μE$m^{-2}s^{-1}$. Attempts were made to grow the culture at 80 μE$m^{-2}s^{-1}$, including very slow acclimation to higher light over many generations. However, the culture would unexpectedly crash, even when it appeared healthy (high F_v/F_M, log phase growth rate) the day before. Nevertheless, our analysis indicates that WH7805 shares attributes of both HLO and LLO traits. The photosynthetic electron transport characteristics are more similar to HLO strains, where transport rates continue to increase under very high actinic light (Fig. 3). Only in cells acclimated to the lowest light treatment (5 μE$m^{-2}s^{-1}$) was a decline in electron transport rate noted at the highest actinic irradiance. Further, while photosynthetic electron transport proteins were more abundant under low light (consistent with LLO strains), proteins involved with carbon concentration and fixation, Fe metabolism, and N metabolism were all more abundant under higher light (consistent with HLO strains; Fig. 5B, Table 1). The combination of traits for coping in both dim and bright light may allow WH7805 to conserve resources by limiting unnecessary carbon and nutrient metabolism proteins when growth is slower in low light, while maintaining the flexibility to have high photosynthetic electron transport rates without incurring photoinhibition when transiently exposed to high light. These features could indicate that WH7805 is a strain that is particularly well adapted to transient conditions or rapid changes in its environment, such as during mixing.

Strains WH8102 and WH8020 fell toward the LLO end of the light response continuum and shared many similar traits. Both strains had highest growth rates at 40 μE m^{-2} s^{-1}. Additionally, proteins involved in light harvesting, electron transport, and carbon fixation were all more abundant under low light, whereas N metabolism proteins were upregulated under higher light in these strains. The only category that differed was Fe proteins, which were upregulated in higher light for WH8020, but not WH8102 (Fig. 6B; Fig. 6C; Table 1). Despite these similarities, the strains showed differences in their relative electron transport rates when exposed to different actinic irradiances (Fig. 3). When grown under low light at 5 μE m^{-2} s^{-1}, strain WH8102 was unable to cope with the highest actinic light levels; however, when grown under the highest irradiance of 80 μE m^{-2} s^{-1}, this strain showed a remarkably robust response to high actinic light consistent with prior studies (37,38,43). In contrast, electron transport in strain WH8020 was relatively similar regardless of growth irradiance, decreasing with increasing actinic irradiance in excess of 250 μE m^{-2} s^{-1} in all but the highest light treatment.

Among the strains we tested, WH8109 falls furthest toward the LLO end of the light response continuum. Its growth rate saturated at ~20 μE m^{-2} s^{-1} (Fig. 2), and photosynthetic electron transport declined with increasing actinic irradiance even when cells were acclimated to higher light levels (Fig. 3). Additionally, proteins in all five categories were more abundant under lower light (Fig. 6A, Table 1).

The light response continuum reflects optimal light responses that are integrated over longer time periods (multiple generations), but does not necessarily imply that strains cannot exist outside of this optimal range. For example, the strains toward the HLO end of the continuum (e.g. PCC7002, WH7803, WH5701) still had competitive growth rates in low light (5 μE$m^{-2}$$s^{-1}$; Fig.

2), and some of the LLO strains could withstand short pulses of very high light when acclimated to high growth irradiance (Fig. 3). The ability of HLO strains to scale protein abundance with irradiance and growth rate (Fig. 7) could enable them to balance photosynthetic electron flow with downstream metabolic demands and allow them to bloom quickly when light increases, such as during stratification. Strains toward the LLO end of the continuum appear to employ the opposite strategy; investing maximum protein resources for growth under lower light conditions (Fig. 7), and in some cases "burning up" when light levels increase, an occurrence that is observed in natural communities from low light environments (63). This could occur if the high light harvesting efficiency of LLO strains causes too many electrons to enter the photosynthetic electron transport chain, resulting in over-reduction of the photosynthetic membrane and the generation of free radicals. This increase in "excitation pressure" could in turn lead to photoinhibition if membrane proteins become damaged by free radicals (Fig. 3) (64).

Light responses, phylogeny, and biogeography

The results presented here raise the question of whether light responses bear any relation to the phylogenetic affiliation of strains, particularly given that spectral preferences do appear linked to phylogeny (6). In this study we tested seven strains from different sub-clusters or clades as classified previously (4) (Table 1). All LLO strains identified in this study were members of marine sub-cluster 5.1A, including WH8109 (clade I), WH8020 (clade II), and WH8102 (clade III). Clades I and II are commonly found in regions that may undergo deep mixing to 200-600 m (14). The apparent optimization of WH8109 and WH8020 for low light could indicate that they have specialized adaptations for the extremely low irradiances that would be encountered during very deep mixing, and could give them a competitive advantage over other cells that require higher irradiances to grow.

In contrast to the LLO strains, no representatives from sub-cluster 5.1A were classified toward the intermediate or HLO end of the light preference continuum. Notably, *Synechococcus* strains WH5701 and PCC7002 are the only two strains tested in this study classified outside of subcluster 5.1, which contains the majority of known marine *Synechococcus* strains (4). To put this diversity into perspective, *Synechococcus* subcluster 5.1 is more closely related to marine *Prochlorococcus* than to either of these two *Synechococcus* strains. Specifically, strain WH5701 is in sub-cluster 5.2 and PCC7002 is an outgroup that does not fit into sub-clusters 5.1 or 5.2 (4). Moreover, strain PCC7002 was originally identified as *Synechococcus* in 1961 based on morphology (e.g., it is a halotolerant, unicellular cyanobacterium with a phycobilisome) rather than based on gene sequence data, and may ultimately be reclassified into a different genus. The other HLO strain WH7803 is a member of sub-cluster 5.1B (clade V), and the intermediate strain WH7805 is a member of sub-cluster 5.1B (clade VI). Although this study's analysis is limited to only one strain per clade, these results suggest that there may be a phylogenetic relationship to light preference among *Synechococcus*, with marine strains in subcluster 5.1a (i.e., clades I-IV) being optimized for lower light, and strains in sub-clusters 5.1B, 5.2, and estuarine strains being optimized for higher light.

It is intriguing that both WH5701 and PCC7002 fell toward the HLO end of the light response continuum given that these strains are both classified as pigment type 1 (i.e., having phycobilisomes consisting of phycocyanin without phycoerythrin, Table 1). Tolerance to higher light in these strains could be related to morphology of their phycobilisomes. Phycobilisome rods can contain either phycocyanin (PC) alone (pigment type 1), or PC plus phycoerythrin (PE, pigment types 2 and 3) (20). Pigment type 2 always binds the chromophores phycoerythrobilin (PEB; max absorption wavelength = 550 nm) and phycouribilin (PUB; max absorption

wavelength = 495 nm) jointly. Pigment type 3 can either bind PEB exclusively, or PEB and PUB together (see reference (20) for a thorough discussion of pigment types). Based on the ratio of PEB:PUB, strains can be further classified into sub-types 3a, 3b, 3c, and 3d(20). Strains belonging to pigment type 2 and 3 have larger antennae with a broader range of wavelength absorption spectra compared to type 1. The tolerance of WH5701 and PCC7002 for high light is consistent with a strategy to avoid absorbing unnecessary light by having smaller antennas. In contrast, PE containing strains (types 2 and 3) necessarily have larger antennas capable of absorbing more wavelengths of light (Fig. 2). This is particularly true of pigment types with higher proportions of blue light-absorbing PUB (3c and 3d), such as WH8109, WH8102, and WH8020, all of which fell toward the LLO end of the light preference continuum in this study (Table 1). While these strains can acclimate to higher growth irradiance by synthesizing less phycobilisome proteins on a cellular basis (Figs. 4-6, Table 1) they have inherently larger photosynthetic cross sections for blue light due to their higher PUB content (Fig. 2), thus with all other factors being equal, photosynthesis saturates at lower irradiances for these strains. In contrast, PC-rich type 1 strains have smaller photosynthetic cross sections for blue light harvesting, and so could experience comparatively less excitation pressure under higher light. This may allow them to avoid photoinhibition in brighter environments because they harvest less light. However, we note that *Synechococcus* with PE-containing antennae (types 2 and 3) are commonly found in high light environments like the Costa Rica Dome (65), and certain strains have been shown to tolerate extremely high light in culture (15), hence the size and composition of the PBS is not the only factor that determines light responses. The ability to quench excitation energy, balance electron flow to avoid photoinhibition, and repair proteins after photodamage occurs likely together give rise to light response phenotypes.

Although closely genetically related to marine *Synechococcus*, the light responses of *Prochlorococcus* differ markedly. *Prochlorococcus* relies on membrane integral chlorophyll binding proteins to form an antenna around PSI, similar to the IsiA proteins in other cyanobacteria (26,27,66). To date only four marine *Synechococcus* strains have been found to retain *isiA* (4), and none of the strains in this study have the gene. Moreover, niche partitioning in *Prochlorococcus* is strongly influenced by irradiance, and high light-adapted and low light-adapted ecotypes show distinct physiological and genetic traits that clearly distinguish the two groups (3). Compared to *Synechococcus*, the more restricted geographical range of *Prochlorococcus*, which is commonly found in permanently stratified waters (7,8) where light levels and nutrient availability are constant over time, may prompt *Prochlorococcus* to evolve to fill high and low light niches (although we note that *Prochlorococcus* is also found in seasonally mixed locations (10,12,67,68)). Despite its global distribution, this study found no strong link between latitude and light response for *Synechococcus* (Fig. 1, Table 1); rather, the patterns seem more closely related to phylogeny and pigment composition (Table 1). Nevertheless, with its broader distributions in both permanently stratified waters and areas of dynamic seasonal mixing, *Synechococcus* as a genus experiences variable light regimes and may benefit from retaining traits that allow each ecotype to survive over a broader range of irradiances, rather than diversifying into more specialized high and low light ecotypes.

Synechococcus seems to fall along a continuum of light responses ranging from low light optimized to high light optimized phenotypes. These responses appear to be linked to phylogeny and pigment composition, where members of marine sub-cluster 5.1a that have higher relative amounts of PUB tend to fall toward the low light optimized end of the spectrum. The global proteomes of all seven strains tested were highly responsive to light intensity, but the only

strongly conserved feature was down-regulation of phycobilisome proteins in higher light. The lack of a clear trend in light response with latitude suggests that other environmental factors, like nutrient demand and temperature preferences, exert equal or greater selective pressure on *Synechococcus* biogeography (6–8,43,69). However, the conserved set of photoacclimation mechanisms found in the genus (state transitions, Hlips, OCPs, etc.), of which each strain uses a different subset, indicates that common light response mechanisms are maintained within the genus overall, and are therefore evolutionarily valuable to the lineage.

Experimental Procedures

Culture conditions. *Synechococcus* strains WH5701, WH7803, WH7805, WH8020, WH8102, WH8109, and PCC7002 were provided by the Waterbury and Mincer laboratories at the Woods Hole Oceanographic Institution. Strains were selected to include representatives from clades that were isolated from different latitudes along a roughly longitudinal transect in the Atlantic Ocean (Fig. 1B), and based on availability of sequenced genomes to facilitate proteomic analyses. Non-axenic cultures were maintained in dilute, semi-continuous batch culture in a temperature controlled growth chamber (23 ^{o}C) under continuous white light provided by a combination of cool-white and grow light (Sylvania Ecologic) fluorescent bulbs. Media consisted of 75% coastal seawater from Martha's Vineyard Sound and 25% MilliQ water with SN nutrient amendments (70) supplemented with vitamin 0.4 nM cyanocobalamin (vitamin B_{12}).

Cultures were grown at 5, 10, 20, 40, and 80 μE m^{-2} s^{-1} for at least 10 generations in semi-continuous batch culture before mid-log phase sampling. These irradiance levels were measured using a quantum/radiameter/photometer (LI-COR Inc., model LI-185B). This range of irradiance levels was selected to encompass conditions under which all of the strains could consistently grow, although we note that several of the strains included here are capable of growth in

irradiances >80 μE m^{-2} s^{-1} (as discussed above). Doubling times were determined from raw fluorescence measurements using the equation $F_f = F_i * 2^{(t/T)}$, where F_f is the final fluorescence value, F_i is the initial fluorescence value, t is the time between initial and final measurements, and T is the doubling time. Growth rate was calculated by multiplying this value by 0.7. For each strain and treatment, the growth rate was calculated using two time points from within the exponential phase of the curve prior to collection of the proteome sample, i.e. after the final subbing for these semi-continuous cultures. Growth rates were similar when calculated based on exponential phase calculations from prior continuous culturing of the cells (typically 3-4 serial transfers in time).

Photosystem II fluorescence. Photosynthetic efficiency was measured on a FIRe Fluorometer (Satlantic) with the blue single turnover flash duration extended to 200 μs as described previously (44). The dark-adapted photosynthetic efficiency (Fv/F_M), the photosynthetic efficiency at a given light level (ΦPSII) and the photosynthetic cross sectional area, σ_{blue}, were determined using a single turnover flash of blue excitation (see reference (36) for a mathematical description of these parameters). Curve fitting was done with the multiple turnover flash algorithm disabled. Three to six measurements were taken on each strain/treatment on different (typically sequential) days while cells remained in exponential growth phase, and the values were averaged. The value of σ_{blue} in units of Ångstroms squared was calculated by multiplying the value in relative by a calibration factor of 2.3. We report values of σ_{blue} to two significant digits to reflect calibration factor uncertainty.

Photosynthesis irradiance curves were conducted at actinic background light levels of 0, 5, 10, 20, 40, 83, 167, 250, 500, and 1000 μE m^{-2} s^{-1} following a 30 sec acclimation period. Thirty

seconds was determined to be sufficient for fluorescence to stabilize before the measurement was taken. Each curve was measured either on the same day or the day immediately preceding collection of the proteome sample. Relative PSII electron transport rate (ETR), which is the product of irradiance and ΦPSII, was plotted against irradiance to provide a qualitative diagnostic metric of photosynthetic efficiency under transient high and low light conditions (Fig. 3). The calculated electron transport rate is considered ‘‘relative’’ because no corrections have been made to account for the partitioning of absorbed light between PSI and PSII in these calculations. Standard error of the computed relative ETR data points were then calculated by multiplying each ETR point with its corresponding standard error values from ΦPSI; however, in all cases the error bars were smaller than the series markers in Fig. 3.

Global proteomics. Proteome samples were collected on 0.2 μm Supor polyestersulfone filters and stored frozen at -80 ^{o}C until analysis. For each strain, one filter sample was collected at each light level. Proteins were processed as described previously (44). Briefly, cell samples were thawed and rinsed from the filters in 100 mM ammonium bicarbonate, split into two technical replicates, sonicated on ice 10 min, and centrifuged. Proteins were precipitated overnight in 100% acetone at -20 ^{o}C, then protein material was resuspended in 6 M urea with 0.1 mM ammonium bicarbonate, reduced with 10 mM dithiothreitol (56 ^{o}C, 450 rpm on a thermomixer for 1 hr), and alkylated with 30 mM iodoacetamide (20 ^{o}C on bench for 1 hr). Proteins were quantified using the Bradford Protein Assay Kit (BioRad) and digested with trypsin (Promega Trypsin Gold; 37 ^{o}C, 400 rpm on a thermomixer overnight) at an enzyme: protein ratio of 1:50. The tryptic peptides were concentrated by evaporation and resuspended in 2% (vol/vol) acetonitrile with 0.2% (vol/vol) formic acid. While deeper proteomes are possible with the use of

detergent-based extractions and alternate chromatographic methods, we find this method to be reproducible and efficient.

Tryptic peptides were analyzed on technical duplicate samples via chromatography and tandem mass spectrometry (LC-MS/MS) on a Q Exactive (QE) Hybrid Quadrupole-Orbitrap Mass Spectrometer (Thermo Scientific). A gradient of 0.1% (vol/vol) formic acid in water and 1.1% (vol/vol) formic acid in acetonitrile was used for the chromatography. Tandem mass spectrometry was performed on the top 15 ions, and ions with a mass to charge ratio from 400 to 2,000 were monitored.

Peptides were identified using the reference genome for each strain with the SEQUEST algorithm within Proteome Discoverer (Thermo). Identification criteria included a protein identification probability of 99%, a peptide identification probability of 95%, and identification of two or more peptides from the protein's sequence (71). Normalized spectral counts for each protein were computed with Scaffold software (Version 4.3.2 Proteome Software), and measurements from the technical duplicates were averaged. Spectral counts refer to the total number of spectra identified with the mass spectrometer for a given protein within a proteome sample(72). In Scaffold, the normalization method sums the unweighted spectral counts for all proteins within each sample, and then applies a small normalization correction to each sample's spectral count proteome so that the sum of spectral counts is equal across the sample set. The method is appropriate when similar amounts of protein are analyzed between samples, as is the case in this study. To be included in our further detailed analysis and discussion, we applied a threshold of four normalized spectral counts summed across treatments in order to exclude rarer proteins detected less frequently.

The complete global proteome dataset meeting the criteria of 4 spectral counts across treatments for each strain is given in the Supplemental Tables 2-8. Proteins involved in light harvesting, photosynthetic electron transport, carbon fixation, iron metabolism, and nitrogen metabolism were identified and sub-selected for comparison in Fig. 4-6, Fig. 2 (column 2) and Table 1 by searching the proteomes for the following terms: photo, chloro, phyco, ribulose, carbon, carboxysome, iron, ferr, nitr, ammo, urea, cyanate, and amino. Iron- containing electron transport chain proteins like PSI, PSII, and cytochrome b6f are listed in the "electron transport chain" category rather than the "iron metabolism" category, although there is clearly overlap between these groups. The normalized spectral data for proteins in these categories was imported into Cluster 3.0 (73), log transformed, centered on mean, and normalized across treatments. Proteins were clustered using the correlation (uncentered) similarity metric and centroid linkage options to generate heatmaps. To determine if proteins in these groups were up- or down-regulated in response to increasing irradiance, the spectral counts under the highest and lowest irradiance treatments were compared.

The global proteomes were analyzed to determine the percent of all proteins that increased or decreased by a factor of 2 or more between the lowest and highest light treatment for each strain. First, the sum of all spectral counts was summed across treatments for each protein, and only proteins with counts above 4 were used in the analysis. The ratio of spectral counts in the low versus high treatment was then calculated, and these ratios were sorted into bins of <0.5, 0.5-2.0, and >2.0. While specific statistical tests are capable of detecting significant changes with greater sensitivity (e.g. Fisher's test) can be applied to various within each strains experiment, the use of 2-fold differences allowed a uniform approach to compare large scale differences across strains

for the purposes of this study. The percentage of proteins in each bin was used to determine the fraction of the proteome that is most responsive to irradiance.

To facilitate analysis in this paper, we have compared cell responses under the highest and lowest growth irradiances tested here, but it is important to recognize that the success of each strain at these irradiances reflects their different optimal growth irradiances. Specifically, the highest irradiance tested (80 μE m^{-2} s^{-1}) is sub-saturating for growth in the HLO strains, but above the optimal growth irradiance for the LLO strains. The comparison therefore provides insight into how each strain would respond under similar light conditions in the water column, rather than about optimal physiological conditions.

Gene identification

High light inducible proteins, photolyases, and orange carotenoid proteins were identified in the seven genomes using BLASTp. Known sequences were blasted against each genome to identify homologous proteins, and these sequences were further blasted against the genomes until no additional sequences were identified. Homology was checked by blasting the new sequences and checking that the best matches confirmed the homology.

Acknowledgements

We thank A. Aicher and J. Waterbury for providing the *Synechococcus* strains. K.R.M.M was supported by an NSF Postdoctoral Fellowship in Biology.

References

1. Flombaum P, Gallegos JL, Gordillo RA, Rincon J, Zabala LL, Jiao N, et al. Present and future global distributions of the marine Cyanobacteria Prochlorococcus and Synechococcus. Proc Natl Acad Sci. 2013 Jun 11;110(24):9824–9.

2. Liu H, Landry MR, Vaulot D, Campbell L. Prochlorococcus growth rates in the central equatorial Pacific: An application of the *f*max approach. J Geophys Res Oceans. 1999 Feb 15;104(C2):3391–9.

3. Rocap G, Larimer FW, Lamerdin J, Malfatti S, Chain P, Ahlgren NA, et al. Genome divergence in two Prochlorococcus ecotypes reflects oceanic niche differentiation. Nature. 2003 Aug 28;424(6952):1042–7.

4. Scanlan DJ, Ostrowski M, Mazard S, Dufresne A, Garczarek L, Hess WR, et al. Ecological Genomics of Marine Picocyanobacteria. Microbiol Mol Biol Rev. 2009 Jun 1;73(2):249–99.

5. Partensky F, Hess WR, Vaulot D. Prochlorococcus, a Marine Photosynthetic Prokaryote of Global Significance. Microbiol Mol Biol Rev. 1999 Mar 1;63(1):106–27.

6. Ahlgren NA, Rocap G. Culture Isolation and Culture-Independent Clone Libraries Reveal New Marine Synechococcus Ecotypes with Distinctive Light and N Physiologies. Appl Environ Microbiol. 2006 Nov 1;72(11):7193–204.

7. Zwirglmaier K, Heywood JL, Chamberlain K, Woodward EMS, Zubkov MV, Scanlan DJ. Basin-scale distribution patterns of picocyanobacterial lineages in the Atlantic Ocean. Environ Microbiol. 2007 May 1;9(5):1278–90.

8. Zwirglmaier K, Jardillier L, Ostrowski M, Mazard S, Garczarek L, Vaulot D, et al. Global phylogeography of marine Synechococcus and Prochlorococcus reveals a distinct partitioning of lineages among oceanic biomes. Environ Microbiol. 2008 Jan 1;10(1):147–61.

9. Hunter-Cevera KR, Post AF, Peacock EE, Sosik HM. Diversity of Synechococcus at the Martha's Vineyard Coastal Observatory: Insights from Culture Isolations, Clone Libraries, and Flow Cytometry. Microb Ecol. 2016;1–14.

10. Mackey KRM, Bristow L, Parks DR, Altabet MA, Post AF, Paytan A. The influence of light on nitrogen cycling and the primary nitrite maximum in a seasonally stratified sea. Prog Oceanogr. 2011 Dec;91(4):545–60.

11. Mackey KRM, Rivlin T, Grossman AR, Post AF, Paytan A. Picophytoplankton responses to changing nutrient and light regimes during a bloom. Mar Biol. 2009 Apr 9;156(8):1531–46.

12. DuRand MD, Olson RJ, Chisholm SW. Phytoplankton population dynamics at the Bermuda Atlantic Time-series station in the Sargasso Sea. Deep Sea Res Part II Top Stud Oceanogr. 2001;48(8–9):1983–2003.

13. Lindell D, Post AF. Ultraphytoplankton succession is triggered by deep winter mixing in the Gulf of Aqaba (Eilat), Red Sea. Limnol Oceanogr. 1995 Sep 1;40(6):1130–41.

14. Post AF, Penno S, Zandbank K, Paytan A, Huse SM, Welch DM. Long Term Seasonal Dynamics of Synechococcus Population Structure in the Gulf of Aqaba, Northern Red Sea. Front Microbiol [Internet]. 2011 Jun 20 [cited 2015 May 26];2. Available from: http://www.ncbi.nlm.nih.gov/pmc/articles/PMC3122069/

15. Kana T, Glibert P. Effect of irradiances up to 2000 μE m− 2 s− 1 on marine Synechococcus WH7803—I. Growth, pigmentation, and cell composition. Deep Sea Res Part Oceanogr Res Pap. 1987;34:497–495.

16. Cohen-Bazire G, Bryant DA. Phycobilisomes: composition and structure [Algae, cyanobacteria]. Bot Monogr USA [Internet]. 1982 [cited 2017 Jan 26]; Available from: http://agris.fao.org/agris-search/search.do?recordID=US8255381

17. Bennett A, Bogorad L. Complementary chromatic adaptation in a filamentous blue-green alga. J Cell Biol. 1973;58(2):419–435.

18. Kana TM, Feiwel NL, Flynn LC. Nitrogen starvation in marine Synechococcus strains: clonal differences in phycobiliprotein breakdown and energy coupling. Mar Ecol-Prog Ser. 1992;88:75–75.

19. Campbell D, Hurry V, Clarke AK, Gustafsson P, Öquist G. Chlorophyll Fluorescence Analysis of Cyanobacterial Photosynthesis and Acclimation. Microbiol Mol Biol Rev. 1998 Sep 1;62(3):667–83.

20. Six C, Thomas J-C, Garczarek L, Ostrowski M, Dufresne A, Blot N, et al. Diversity and evolution of phycobilisomes in marine Synechococcus spp.: a comparative genomics study. Genome Biol. 2007;8(12):R259.

21. Bidigare R, Marra J, Dickey T, Iturriaga R, Baker K, Smith R, et al. Evidence for phytoplankton succession and chromatic adaptation in the Sargasso Sea during spring 1985'. Mar Ecol Prog Ser. 1990;60:113–122.

22. Mullineaux CW, Tobin MJ, Jones GR. Mobility of photosynthetic complexes in thylakoid membranes. Nature. 1997 Nov 27;390(6658):421–4.

23. McConnell MD, Koop R, Vasil'ev S, Bruce D. Regulation of the Distribution of Chlorophyll and Phycobilin-Absorbed Excitation Energy in Cyanobacteria. A Structure-Based Model for the Light State Transition. Plant Physiol. 2002 Nov 1;130(3):1201–12.

24. Biggins J, Bruce D. Regulation of excitation energy transfer in organisms containing phycobilins. Photosynth Res. 1989 Apr;20(1):1–34.

25. Kirilovsky D, Kerfeld CA. The orange carotenoid protein in photoprotection of photosystem II in cyanobacteria. Biochim Biophys Acta BBA - Bioenerg. 2012 Jan;1817(1):158–66.

26. Bibby TS, Nield J, Barber J. Iron deficiency induces the formation of an antenna ring around trimeric photosystem I in cyanobacteria. Nature. 2001;412(6848):743–745.

27. Boekema EJ, Hifney A, Yakushevska AE, Piotrowski M, Keegstra W, Berry S, et al. A giant chlorophyll–protein complex induced by iron deficiency in cyanobacteria. Nature. 2001 Aug 16;412(6848):745–8.

28. Funk C, Vermaas W. A cyanobacterial gene family coding for single-helix proteins resembling part of the light-harvesting proteins from higher plants. Biochemistry (Mosc). 1999;38(29):9397–9404.

29. Montané M-H, Kloppstech K. The family of light-harvesting-related proteins (LHCs, ELIPs, HLIPs): was the harvesting of light their primary function? Gene. 2000 Nov 27;258(1–2):1–8.

30. Xu H, Vavilin D, Funk C, Vermaas W. Small Cab-like proteins regulating tetrapyrrole biosynthesis in the cyanobacterium Synechocystis sp. PCC 6803. Plant Mol Biol. 2002 May 1;49(2):149–60.

31. Komenda J, Sobotka R. Cyanobacterial high-light-inducible proteins — Protectors of chlorophyll–protein synthesis and assembly. Biochim Biophys Acta BBA - Bioenerg. 2016 Mar;1857(3):288–95.

32. Ng W-O, Zentella R, Wang Y, Taylor J-SA, Pakrasi HB. phrA, the major photoreactivating factor in the cyanobacterium Synechocystis sp. strain PCC 6803 codes for a cyclobutane-pyrimidine-dimer-specific DNA photolyase. Arch Microbiol. 2000 May 3;173(5–6):412–7.

33. Hagman Å, Shi L-X, Rintamäki E, Andersson B, Schröder WP. The Nuclear-Encoded PsbW Protein Subunit of Photosystem II Undergoes Light-Induced Proteolysis. Biochemistry (Mosc). 1997 Oct 1;36(42):12666–71.

34. Gupta AS, Heinen JL, Holaday AS, Burke JJ, Allen RD. Increased resistance to oxidative stress in transgenic plants that overexpress chloroplastic Cu/Zn superoxide dismutase. Proc Natl Acad Sci. 1993 Feb 15;90(4):1629–33.

35. Muramatsu M, Hihara Y. Acclimation to high-light conditions in cyanobacteria: from gene expression to physiological responses. J Plant Res. 2012 Jan 1;125(1):11–39.

36. Mackey KRM, Paytan A, Grossman AR, Bailey S. A photosynthetic strategy for coping in a high-light, low-nutrient environment. Limnol Oceanogr. 2008;53(3):900–13.

37. Bailey S, Melis A, Mackey KRM, Cardol P, Finazzi G, van Dijken G, et al. Alternative photosynthetic electron flow to oxygen in marine Synechococcus. Biochim Biophys Acta BBA - Bioenerg. 2008 Mar;1777(3):269–76.

38. Grossman AR, Mackey KRM, Bailey S. A Perspective on Photosynthesis in the Oligotrophic Oceans: Hypotheses Concerning Alternate Routes of Electron Flow1. J Phycol. 2010 Aug 1;46(4):629–34.

39. Mehler AH. Studies on reactions of illuminated chloroplasts: I. Mechanism of the reduction of oxygen and other hill reagents. Arch Biochem Biophys. 1951 Aug;33(1):65–77.

40. Munekage Y, Hashimoto M, Miyake C, Tomizawa K-I, Endo T, Tasaka M, et al. Cyclic electron flow around photosystem I is essential for photosynthesis. Nature. 2004 Jun 3;429(6991):579–82.

41. Moore LR, Post AF, Rocap G, Chisholm SW. Utilization of different nitrogen sources by the marine cyanobacteria Prochlorococcus and Synechococcus. Limnol Oceanogr. 2002 Jul 1;47(4):989–96.

42. Penno S, Lindell D, Post AF. Diversity of Synechococcus and Prochlorococcus populations determined from DNA sequences of the N-regulatory gene ntcA. Environ Microbiol. 2006 Jul 1;8(7):1200–11.

43. Mackey KRM, Paytan A, Caldeira K, Grossman AR, Moran D, McIlvin M, et al. Effect of Temperature on Photosynthesis and Growth in Marine Synechococcus spp. Plant Physiol. 2013 Oct 1;163(2):815–29.

44. Mackey KRM, Post AF, McIlvin MR, Cutter GA, John SG, Saito MA. Divergent responses of Atlantic coastal and oceanic Synechococcus to iron limitation. Proc Natl Acad Sci. 2015 Aug 11;112(32):9944–9.

45. Glover HE, Prézelin BB, Campbell L, Campbell M, Garside C. A nitrate-dependent Synechococcus bloom in surface Sargasso Sea water. Nature. 1988 Jan 14;331(6152):161–3.

46. Mazard S, Ostrowski M, Partensky F, Scanlan DJ. Multi-locus sequence analysis, taxonomic resolution and biogeography of marine Synechococcus. Environ Microbiol. 2012 Feb 1;14(2):372–86.

47. Saito MA, Rocap G, Moffett JW. Production of cobalt binding ligands in a Synechococcus feature at the Costa Rica upwelling dome. Limnol Oceanogr. 2005 Jan 1;50(1):279–90.

48. Sohm JA, Ahlgren NA, Thomson ZJ, Williams C, Moffett JW, Saito MA, et al. Co-occurring Synechococcus ecotypes occupy four major oceanic regimes defined by temperature, macronutrients and iron. ISME J [Internet]. 2015 Jul 24 [cited 2015 Jul 30]; Available from: http://www.nature.com/ismej/journal/vaop/ncurrent/full/ismej2015115a.html

49. Marshall HL, Geider RJ, Flynn KJ. A mechanistic model of photoinhibition. New Phytol. 2000 Feb 1;145(2):347–59.

50. Mattoo AK, Hoffman-Falk H, Marder JB, Edelman M. Regulation of protein metabolism: Coupling of photosynthetic electron transport to in vivo degradation of the rapidly metabolized 32-kilodalton protein of the chloroplast membranes. Proc Natl Acad Sci. 1984 Mar 1;81(5):1380–4.

51. Six C, Finkel ZV, Irwin AJ, Campbell DA. Light Variability Illuminates Niche-Partitioning among Marine Picocyanobacteria. PLOS ONE. 2007 Dec 19;2(12):e1341.

52. MacIntyre HL, Kana TM, Geider RJ. The effect of water motion on short-term rates of photosynthesis by marine phytoplankton. Trends Plant Sci. 2000 Jan 1;5(1):12–7.

53. Mella-Flores D, Six C, Ratin M, Partensky F, Boutte C, Le Corguillé G, et al. Prochlorococcus and Synechococcus have Evolved Different Adaptive Mechanisms to Cope with Light and UV Stress. Front Microbiol [Internet]. 2012 Aug 8 [cited 2015 Jul 31];3. Available from: http://www.ncbi.nlm.nih.gov/pmc/articles/PMC3441193/

54. Berg GM, Shrager J, Dijken GV, Mills MM, Arrigo KR, Grossman AR. Responses of psbA, hli and ptox genes to changes in irradiance in marine Synechococcus and Prochlorococcus. Aquat Microb Ecol. 2011;65(1):1–14.

55. Shi L-X, Lorković ZJ, Oelmüller R, Schröder WP. The Low Molecular Mass PsbW Protein Is Involved in the Stabilization of the Dimeric Photosystem II Complex in Arabidopsis thaliana. J Biol Chem. 2000 Dec 1;275(48):37945–50.

56. Sakata S, Mizusawa N, Kubota-Kawai H, Sakurai I, Wada H. Psb28 is involved in recovery of photosystem II at high temperature in Synechocystis sp. PCC 6803. Biochim Biophys Acta BBA - Bioenerg. 2013 Jan;1827(1):50–9.

57. Dupont CL, Neupane K, Shearer J, Palenik B. Diversity, function and evolution of genes coding for putative Ni-containing superoxide dismutases. Environ Microbiol. 2008 Jul 1;10(7):1831–43.

58. Saito MA, McIlvin MR, Moran DM, Goepfert TJ, DiTullio GR, Post AF, et al. Multiple nutrient stresses at intersecting Pacific Ocean biomes detected by protein biomarkers. Science. 2014 Sep 5;345(6201):1173–7.

59. Aguirre JD, Clark HM, McIlvin M, Vazquez C, Palmere SL, Grab DJ, et al. A Manganese-rich Environment Supports Superoxide Dismutase Activity in a Lyme Disease Pathogen, Borrelia burgdorferi. J Biol Chem. 2013 Mar 22;288(12):8468–78.

60. Wilson A, Punginelli C, Gall A, Bonetti C, Alexandre M, Routaboul J-M, et al. A photoactive carotenoid protein acting as light intensity sensor. Proc Natl Acad Sci. 2008 Aug 19;105(33):12075–80.

61. Bailey S, Grossman A. Photoprotection in Cyanobacteria: Regulation of Light Harvesting†. Photochem Photobiol. 2008 Nov 1;84(6):1410–20.

Wiley-Blackwell and Society for Applied Microbiology

62. Mullineaux CW. Excitation energy transfer from phycobilisomes to Photosystem I in a cyanobacterium. Biochim Biophys Acta BBA - Bioenerg. 1992 Jun 19;1100(3):285–92.

63. Gerla DJ, Mooij WM, Huisman J. Photoinhibition and the assembly of light□limited phytoplankton communities. Oikos. 2011 Feb 21;3(120):359–68.

64. Adir N, Zer H, Shochat S, Ohad I. Photoinhibition – a historical perspective. Photosynth Res. 2003 Jun 1;76(1–3):343.

65. Ahlgren NA, Noble A, Patton AP, Roache-Johnson K, Jackson L, Robinson D, et al. The unique trace metal and mixed layer conditions of the Costa Rica upwelling dome support a distinct and dense community of Synechococcus. Limnol Oceanogr. 2014 Nov 1;59(6):2166–84.

66. Bibby TS, Mary I, Nield J, Partensky F, Barber J. Low-light-adapted Prochlorococcus species possess specific antennae for each photosystem. Nature. 2003 Aug 28;424(6952):1051–4.

67. Malmstrom RR, Coe A, Kettler GC, Martiny AC, Frias-Lopez J, Zinser ER, et al. Temporal dynamics of Prochlorococcus ecotypes in the Atlantic and Pacific oceans. ISME J. 2010 Oct;4(10):1252–64.

68. Bryant JA, Aylward FO, Eppley JM, Karl DM, Church MJ, DeLong EF. Wind and sunlight shape microbial diversity in surface waters of the North Pacific Subtropical Gyre. ISME J. 2016 Jun;10(6):1308–22.

69. Pittera J, Humily F, Thorel M, Grulois D, Garczarek L, Six C. Connecting thermal physiology and latitudinal niche partitioning in marine Synechococcus. ISME J. 2014 Jun;8(6):1221–36.

70. Waterbury JB, Watson SW, Valois FW, Franks DG. Biological and ecological characterization of the marine unicellular cyanobacterium Synechococcus. Can Bull Fish Aquat Sci. 1986;214:120.

71. Keller A, Nesvizhskii AI, Kolker E, Aebersold R. Empirical Statistical Model To Estimate the Accuracy of Peptide Identifications Made by MS/MS and Database Search. Anal Chem. 2002 Oct 1;74(20):5383–92.

72. Lundgren DH, Hwang S-I, Wu L, Han DK. Role of spectral counting in quantitative proteomics. Expert Rev Proteomics. 2010 Feb;7(1):39–53.

73. de Hoon MJL, Imoto S, Nolan J, Miyano S. Open source clustering software. Bioinformatics. 2004 Jun 12;20(9):1453–4.

74. Marine Synechococcus | Roscoff Culture Collection [Internet]. [cited 2017 Mar 3]. Available from: http://roscoff-culture-collection.org/strains/shortlists/taxonomic-groups/marine-synechococcus?items_per_page=20&order=field_pigment_phenotype&sort=desc

Figure and Table Captions

Table 1: Strain taxonomy, pigment type, and collection information, and photoacclimation gene and protein abundances. Taxonomic classifications are based on (4,6) and pigment types are based on (20,74). Proteins in the categories light harvesting, photosynthetic electron transport, carbon fixation, iron metabolism, and nitrogen metabolism were enumerated based on whether they were more abundant under the high or low light treatments. A rating of "Low" (blue) indicates that proteins in that category increased in abundance under low light, whereas a rating of "High" (red) indicates those proteins became more abundant under high light. Percentages in parentheses show the fraction of proteins in that category that followed the indicated trend. For example, in strain WH8109, 88% of the light harvesting proteins were more abundant under low light.

Fig. 1: (A) Schematic showing typical depth distributions of *Synechococcus* and HL and LL *Prochlorococcus* in a stratified water column where light intensity declines and nitrogen availability increases with depth. (B) Map showing locations of strain isolation in the North Atlantic Ocean. Exact latitude and longitude coordinates are given in Table 1. Strains labeled in pink contain phycoerythrin. Note that PCC7002 is not oceanic having been isolated from a coastal fish pen.

Fig. 2: (First column) Protein extracts of *Synechococcus* strains show changes in light harvesting pigments under different irradiances and the range of pigment types across strains. (Second column) Spectral counts of phycobilisome proteins under different irradiances. These proteins are among the most abundant in *Synechococcus* proteome samples. Proteins are identified in the heatmaps in Fig. 4-6 (“light harvesting” category shown in pink), and each different color in the

graph indicates a different protein designated in the corresponding heatmap of each strain in order of most to least abundant. Changes in abundance are not absolute and are moderately compressed by dynamic exclusion algorithms for recurring (abundant) peptides. (Third column) Photosynthetic cross section of PSII (σ_{blue}) under dark and dim (5 μE m^{-2} s^{-1}) actinic light conditions for cultures grown under different irradiances. Error bars show standard error. (Fourth column) Growth rates of *Synechococcus* strains over different irradiances. * indicates no sample. For WH8020 this was because the yield was too low to accurately measure σ_{blue} at 80 μE m^{-2} s^{-1}.

Fig. 3: Relative photosynthetic electron transport rate (ETR) of *Synechococcus* strains under exposure to 30 seconds of irradiances up to 1000 μE m^{-2} s^{-1}. Relative ETR is the product of irradiance and ΦPSII, and gives a qualitative metric of photosynthetic efficiency under short-term high and low light conditions (short-term acclimation). The rate is considered ‘‘relative’’ because no corrections are made to account for absorbed light partitioning between PSI and PSII. Standard error bars based on 3-6 replicate light curve measurements are smaller than the marker labels. Legend shows growth irradiance.

Fig. 4: Relative abundance of selected proteins from the (A) *Synechococcus* WH7803 and (B) *Synechococcus* WH5701 proteomes, showing protein categories of light harvesting (pink), photosynthetic electron transport (green), carbon fixation (blue), Fe metabolism (orange), and N metabolism (black). Data are log transformed, centered on mean, and normalized across treatments. Yellow and blue indicate higher and lower relative protein abundance respectively, relative to each protein’s mean abundance across treatments. Proteins are clustered based on abundance across conditions and are ordered from top to bottom based on clustering.

Fig. 5: Relative abundance of selected proteins from the (A) *Synechococcus* PCC7002 and (B) *Synechococcus* WH7805 proteomes, showing protein categories of light harvesting (pink), photosynthetic electron transport (green), carbon fixation (blue), Fe metabolism (orange), and N metabolism (black). Data are log transformed, centered on mean, and normalized across treatments. Yellow and blue indicate higher and lower relative protein abundance respectively, relative to each protein's mean abundance across treatments. Proteins are clustered based on abundance across conditions and are ordered from top to bottom based on clustering.

Fig. 6: Relative abundance of selected proteins from the (A) *Synechococcus* WH8109, (B) *Synechococcus* WH8020, and (C) *Synechococcus* WH8102 proteomes, showing protein categories of light harvesting (pink), photosynthetic electron transport (green), carbon fixation (blue), Fe metabolism (orange), and N metabolism (black). Data are log transformed, centered on mean, and normalized across treatments. Yellow and blue indicate higher and lower relative protein abundance respectively, relative to each protein's mean abundance across treatments. Proteins are clustered based on abundance across conditions and are ordered from top to bottom based on clustering.

Fig. 7: The fraction of each strain's proteome upregulated under low (blue bars) and high light (yellow bars).

Fig. 8: Abundance of oxidative stress protection proteins, Psb28 and SODs. * indicates no sample.

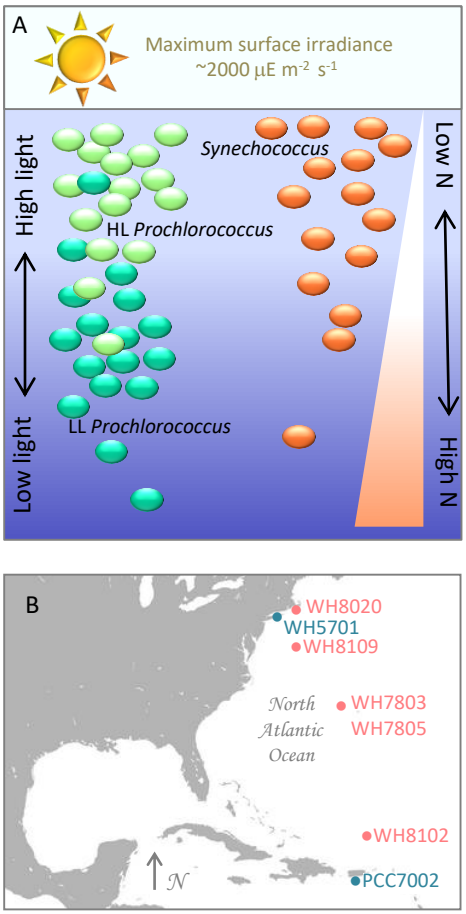

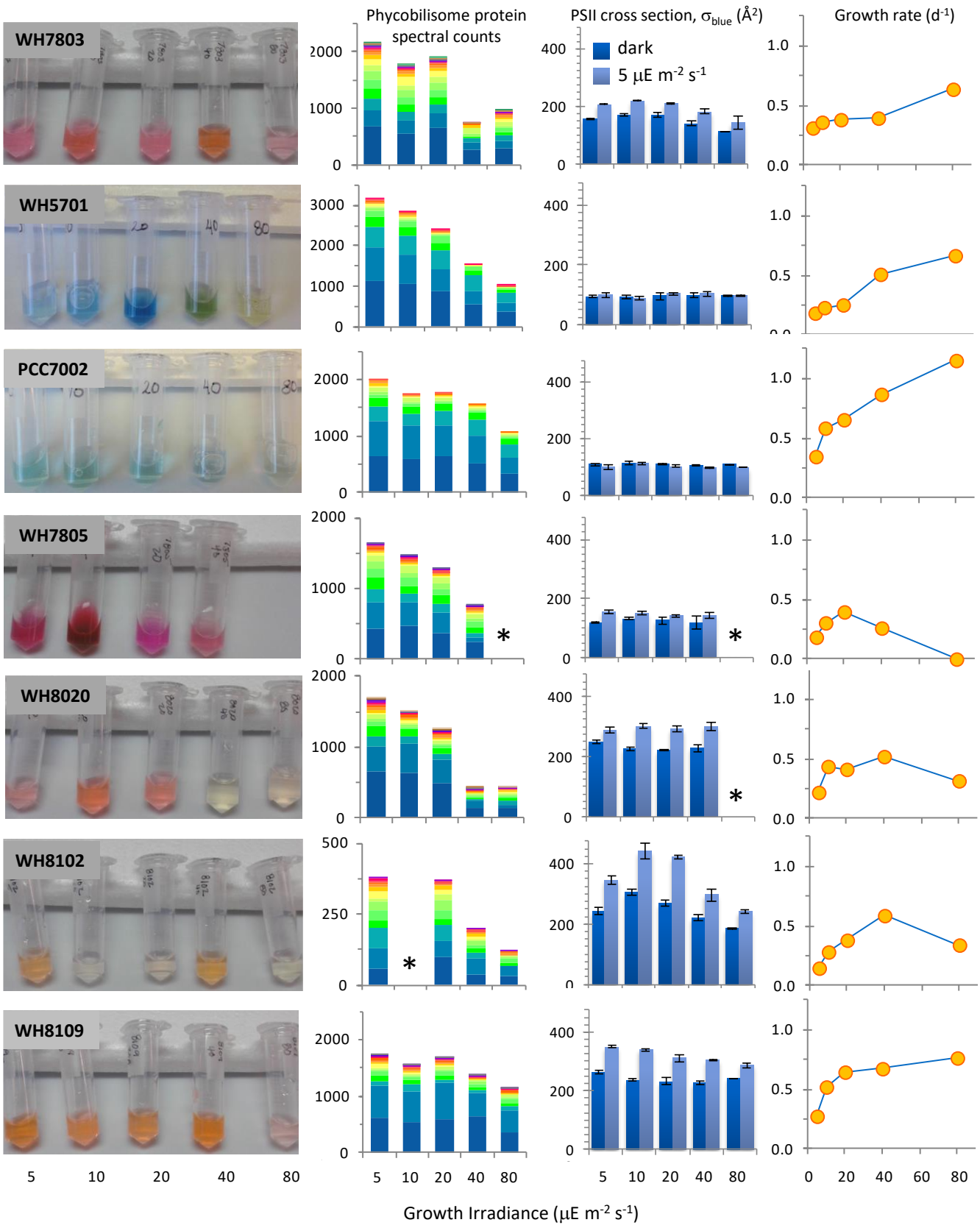

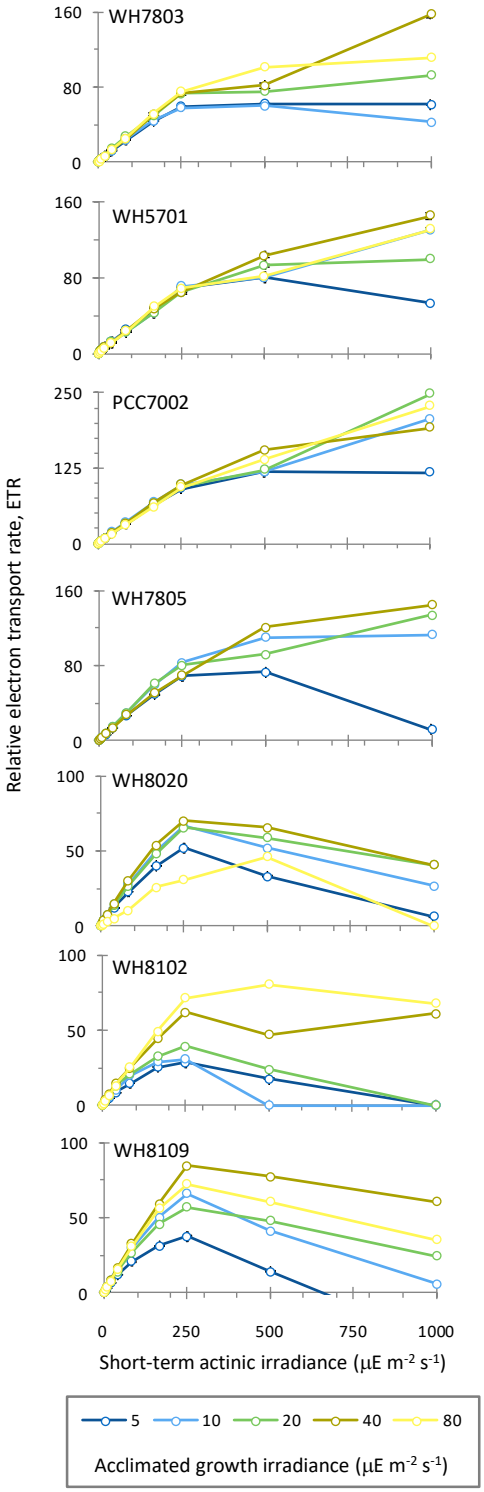

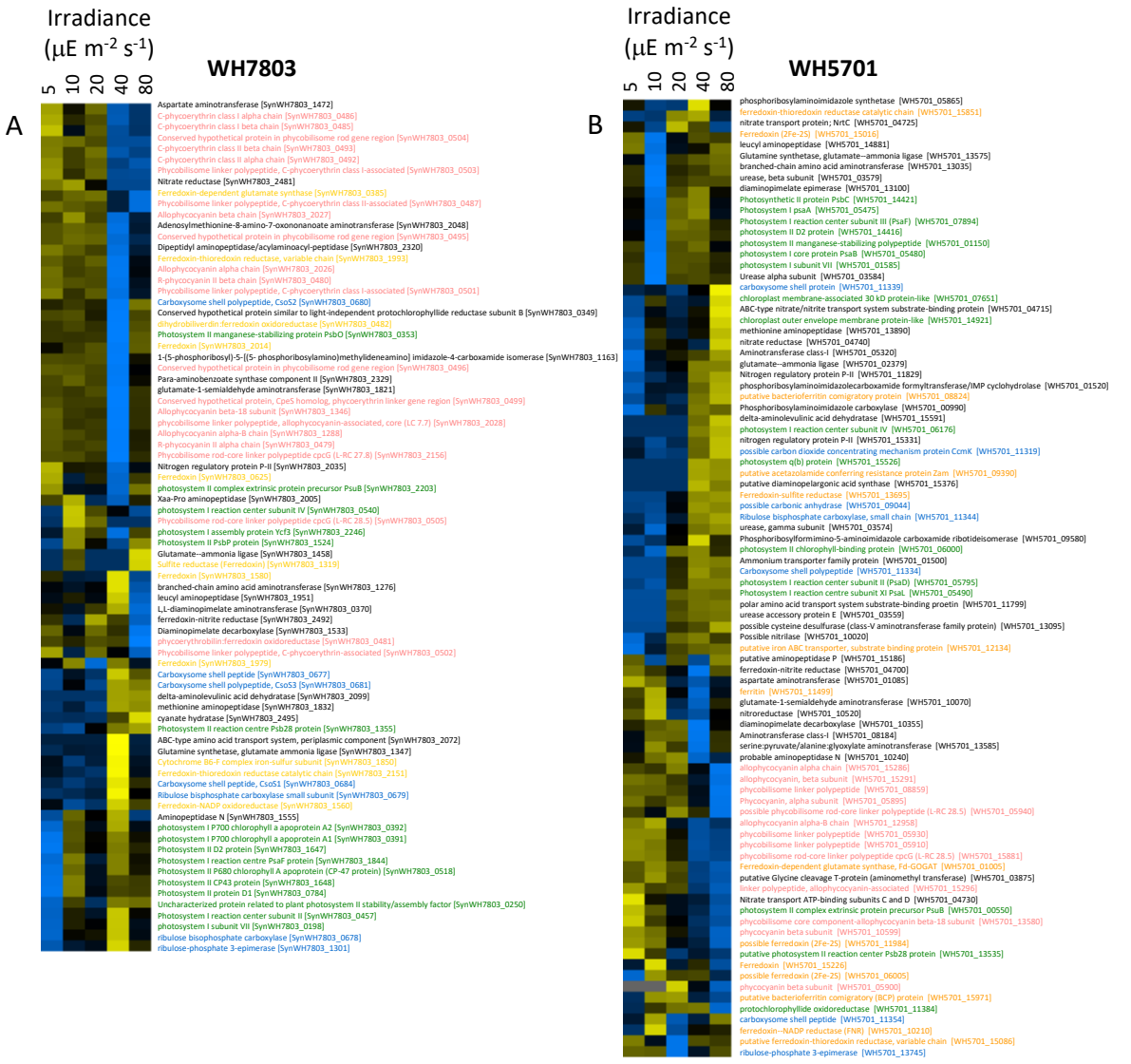

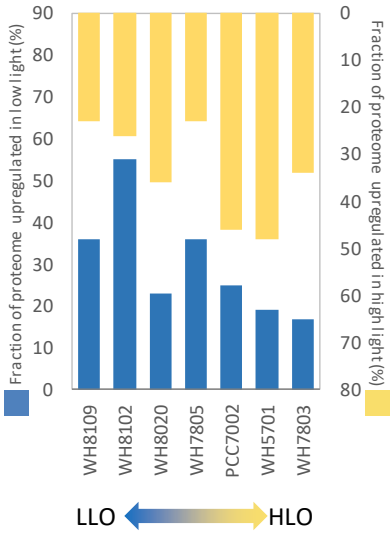

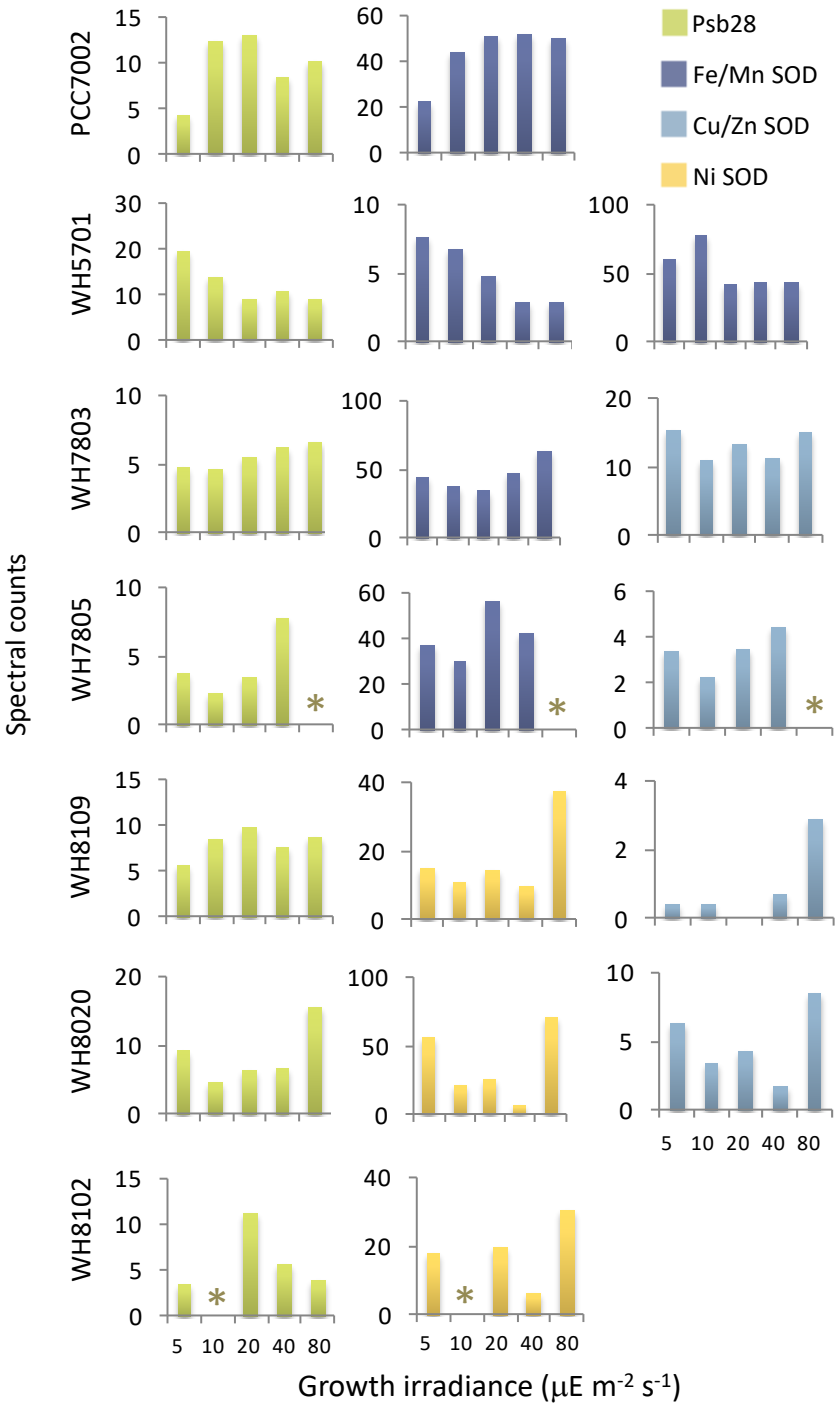

Strain	Classification based on growth rate	Taxonomy	Pigment Type	Isolation details	# *hli* genes in genome	# photolyase genes in genome	# orange carotenoid protein genes in genome	Proteome upregulated in low light*	Proteome upregulated in high light*	light harvesting	Photo-synthetic electron transport	carbon fixation	Fe metabolism	N metabolism
WH8109	LLO	Marine sub-cluster 5.1A, clade IIa	3 d	39.47°N, 70.45°W; northwestern Atlantic Ocean slope water; June 1981	8	5	0	208 (36%)	133 (23%)	Low (88%)	Low (95%)	Low (71%)	Low (75%)	Low (87%)
WH8102	LLO	Marine sub-cluster 5.1A, clade, IIIa	3c	22.495°N, 65.6°W; surface; Sargasso Sea, North Atlantic, from Oceanus cruise 92; March 15, 1981	9	4	1	129 (55%)	61 (26%)	Low (93%)	Low (55%)	Low (75%)	Low (83%)	High (73%)
WH8020	LLO	Marine sub-cluster 5.1A, clade Ia	3d	38.68°N, 69.3°W; 50 m depth; northwestern Atlantic Ocean slope water; June 26, 1980	12	4	1	124 (23%)	197 (36%)	Low (100%)	Low (71%)	Low (60%)	High (83%)	High (55%)
WH7805	intermediate	Marine sub-cluster 5.1B, clade VIc	2	33.7413°N, 67.5°W; Sargasso Sea, North Atlantic Ocean; June 30, 1978	9	4	1	268 (36%)	174 (23%)	Low (75%)	Low (89%)	High (80%)	High (56%)	High (57%)
PCC7002	HLO	Estuarine	1	17.97°N, 67.05°W; onshore, marine fish pen mud sample; Magueyes Island, La Parguera, Puerto Rico; Caribbean Sea, North Atlantic Ocean; 1961	4	3	3	152 (25%)	287 (46%)	Low (58%)	Low (82%)	Low (88%)	High (63%)	Low (73%)
WH5701	HLO	Marine sub-cluster 5.2	1	41.19°N 73.06°W; in sand with clams; Long Island Sound, North Atlantic Ocean; 1958	15	5	1	148 (19%)	365 (48%)	Low (100%)	High (82%)	High (71%)	Low (54%)	High (69%)
WH7803	HLO	Marine sub-cluster 5.1B, clade V	3a	33.7423°N 67.4913°W; 25 m depth; Sargasso Sea, North Atlantic Ocean; 1978	9	4	1	109 (17%)	213 (34%)	Low (100%)	High (81%)	High (86%)	High (55%)	High (55%)

* Indicates the number and percent of detected proteins in the global proteomes for which the ratio of spectral counts in low light to high light was either greater than 2 (indicating proteins that are more abundant in low light) or less than 0.5 (indicating proteins that are more abundant in high light). Ratios between 0.5-2 indicate smaller changes in protein abundance between low and high light, and include proteins that are less sensitive to irradiance (see Supplemental Fig. 1).